Acoustic dispersion of $(NH_3C_2H_5)_2MnCl_4$ near the structural phase transition at 226 K

A. V. Kityk,* W. Schranz, A. Fuith, D. Havlik, V. P. Sopronyuk,* and H. Warhanek
Institut für Experimentalphysik, Universität Wien, Strudlhofgasse 4, 1090 Wien, Austria
(Received 21 August 1995)

The anomaly in the longitudinal elastic constant C_{33} of a $(NH_3C_2H_5)_2MnCl_4$ layered compound around the structural phase transition at $T_2=226$ K was investigated by the ultrasonic method ($f=15$ MHz) and by low frequency dynamic mechanical analysis ($f=0.5-12$ Hz). The present results show a very pronounced dispersion of the longitudinal acoustic modes which are explained in the frame of a phenomenological model including both the effect of temperature fluctuations (isothermal-adiabatic crossover) and order-parameter relaxation. The temperature dependence of the order-parameter relaxation time has been determined from ultrasonic measurements as $\tau_\eta=\tau_0/(T_2-T)$, with $\tau_0=4.5\times10^{-10}$ s K. This value explains the absence of the negative dip anomaly in previous Brillouin scattering experiments. The thermal relaxation time is of the order of $\tau_{th}\approx0.1$ s, and is strongly dependent on sample thickness.

I. INTRODUCTION

Crystals of ethylamin tetrachloromanganate $(NH_3C_2H_5)_2MnCl_4$ (EAMC) belong to the large family of $(C_nH_{2n+1}NH_3)_2MnCl_4$ $(n<5)$ layer structured compounds. They undergo similarly to other members of this group several phase transitions,[1] i.e.,

δ	T_3	γ	T_2	β	T_1	α
	47 K		226 K		424 K	

with the space groups α-$I4/mmm$ $(D_{4h}^{17},Z=1)$ β-$Abma$ $(D_{2h}^{18},Z=2)$, γ-$Pbca$ $(D_{2h}^{15},Z=4)$, δ-$P2_1/b$ (C_{2h}^5). The crystal structure of these compounds is built up by perovskite $MnCl_4$ layers with organic $C_2H_5NH_3^+$ chains, forming hydrogen bonds N-H$\cdots$Cl with the layers. Within one layer the $MnCl_4$ octahedra are connected through four Cl atoms. Interlayer bonding is realized by van der Waals forces, acting between the ends of carbon chains. This leads to a lower elastic rigidity in the direction perpendicular to the layers and a perfect cleavage plane parallel to the xy plane.

All phase transitions in EAMC are caused mainly by the reorientations of the $MnCl_6$ octahedra.[2] Previous ultrasonic,[3] Brillouin scattering, and linear birefringence investigations[4] revealed that the phase transitions at T_1 and T_3 are of second order while the transition at T_2 is probably of first order and very close to a second-order-type transition. The behavior of several acoustic modes near the structural phase transition at $T=T_2$ has been investigated in EAMC with Brillouin scattering.[4] It was shown that, contrary to the predictions of Landau theory, practically no longitudinal acoustic phonon softened in the vicinity of T_2. Only for the C_{11} mode a small decrease was observed around T_2. Therefore the authors have suggested[4] that the forces in the xy plane are changing more strongly than the forces between the layers due to the big anisotropy of the crystal.

However, it is possible to give a quite different explanation for the results obtained from Brillouin scattering measurements, i.e., by taking into account that the strength of the softening of the acoustic phonons near the phase transition may depend on the measuring frequency. Particularly the Brillouin scattering technique yields the elastic constants at high frequencies ($f\approx10^{10}$ Hz) and the acoustic anomalies near the phase transition which are caused by a Landau-Khalatnikov mechanism may be essentially damped if the condition $\omega\tau_\eta\gg1$ (τ_η is the relaxation time for soft mode) is fulfilled. In this case an increase in the softening for longitudinal acoustic phonons would be expected for lower measurement frequencies. In the present work these phenomena are investigated in EAMC crystals near the structural phase transition at $T=T_2$ by using ultrasound ($f=10^7$ Hz) and dynamical mechanical analysis ($f=0.5-12$ Hz) (DMA 7, PERKIN ELMER) techniques. The obtained results are discussed within the framework of the phenomenological Landau theory including a relaxational behavior of the order parameter and temperature fluctuations.

II. EXPERIMENTAL PROCEDURE

Single crystals of EAMC were grown by slow evaporation of water from an aqueous solution of $NH_3C_2H_5Cl$ and $MnCl_2\times4H_2O$ salts, taken in stoichiometric ratio at about 300 K. These compounds usually crystallize in the form of platelets with the c axis perpendicular to the cleavage plane. The samples were selected under a polarizing microscope and only monodomain samples were used for the measurements. We use the standard crystallographic orientation:[3] for the γ phase, $a=7.325$ Å, $b=7.151$ Å, and $c=22.08$ Å. For the ultrasonic measurements the platelet-shaped samples had a typical size of $4\times4\times3$ mm^3. The longitudinal and transverse ultrasonic waves were excited in the sample by $LiNbO_3$ transducers at frequencies of 15 and 10 MHz, respectively. The wave velocities were measured by the pulse-echo overlap method[5] with a relative accuracy of about $10^{-4}-10^{-5}$. The accuracy of the absolute velocity was about 0.5%. The ultrasonic attenuation was determined from the decay rate of the pulse echoes with an accuracy of about 10%.

The low-frequency elastic measurements were performed by the three-point bending method using a dynamic me-

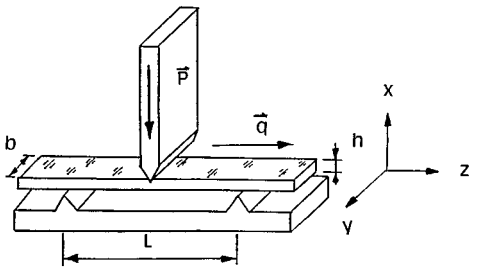

FIG. 1. Three-point bending geometry.

chanical analyzer (DMA 7-PERKIN ELMER). The apparatus works in the frequency range $f=0.01-50$ Hz. In the present experiment we have measured the low-frequency elastic constants in the region $f=0.5-12$ Hz. The sample geometry for the three-point bending method is presented in Fig. 1. The relation between the effective spring constant k measured by the DMA 7 and Young's modulus is determined by the following equation:[6]

$$k=Y(\mathbf{q})4b\left(\frac{h}{L}\right)^3\left[1+1.5\left(\frac{h}{L}\right)^2\frac{Y(\mathbf{q})}{G(\mathbf{pq})}\right]^{-1}. \qquad (1)$$

The geometrical parameters b, h, and L are shown in Fig. 1. $Y(\mathbf{q})$ is Young's modulus along the $\mathbf{q}$ direction, and $G(\mathbf{pq})$ is the shear modulus. Since the values of $Y(\mathbf{q})$ and $G(\mathbf{pq})$ are of the same order and the ratio $(h/L)^2\approx 0.01$ in our measurements we can neglect the second contribution in Eq. (1). In this case the measured effective spring constant k is simply proportional to Young's modulus $Y(\mathbf{q})$. Since the absolute accuracy of these measurements is usually not better than 20% the corresponding results will be presented in a relative form for the real $[C_r'(\mathbf{q})=Y'(\mathbf{q})/Y_0'(\mathbf{q})]$ and the imaginary $[C_r''(\mathbf{q})=C_r'(\mathbf{q})\tan\delta]$ parts of the effective complex elastic constant $C_r^*(\mathbf{q})$. The elastic measurements have been performed with the rate of temperature change of about 1 K/min.

The dielectric measurements have been performed with a Hewlett-Packard 4192 A LF Impedance Analyzer working in the frequency range between 1 kHz and 10 MHz.

III. EXPERIMENTAL RESULTS

A. Ultrasonic and dielectric measurements

The temperature dependences of the elastic constant C_{33} and the corresponding attenuation constant α_{33} (longitudinal mode, $\mathbf{q}\|\mathbf{c}$, $\mathbf{e}\|\mathbf{c}$, where $\mathbf{q}=(0,0,10^3\ \mathrm{cm}^{-1})$ is the ultrasonic wave vector and $\mathbf{e}$ is the polarization of the wave) are shown in Figs. 2(a) and 2(b), respectively. In the β phase ($T>T_2$) the absolute value of C_{33} is in good agreement with the results of Brillouin scattering measurements.[4]

In the vicinity of the phase transition at T_2 a steplike decrease of C_{33} ($\Delta C_{33}/C_{33}\approx 4.6\%$) was observed. Consequently the temperature behavior of C_{33} near T_2 measured at ultrasonic frequencies differs drastically from the Brillouin scattering data [Fig. 2(a)].[4] The clear softening of C_{33} at ultrasonic frequencies is accompanied also by a remarkable increase of the attenuation α_{33} at T_2 [Fig. 2(b)].

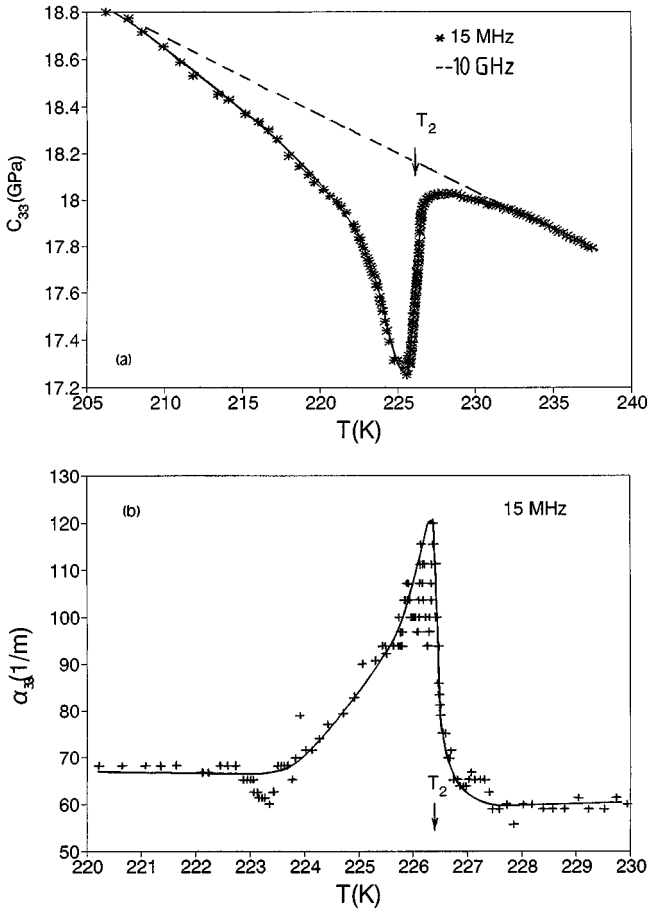

FIG. 2. Temperature dependence of the (a) elastic constant C_{33}; (*) ultrasound data ($f=15$ MHz), (- -) Brillouin scattering data ($f=10$ GHz) of Ref. 4. (b) The corresponding attenuation α_{33} measured by ultrasound.

Contrary to the C_{33} mode the temperature behavior of the transverse acoustic mode $C_{55}(\mathbf{q}\|\mathbf{c},\mathbf{e}\|\mathbf{a})$ is characterized only by a clear kink in the vicinity of T_2 (Fig. 3) with no anomaly in the corresponding attenuation α_{55}. The same character as for the temperature dependence of C_{55} near T_2 is obtained for the dielectric permittivity ϵ_{33} (Fig. 4). The

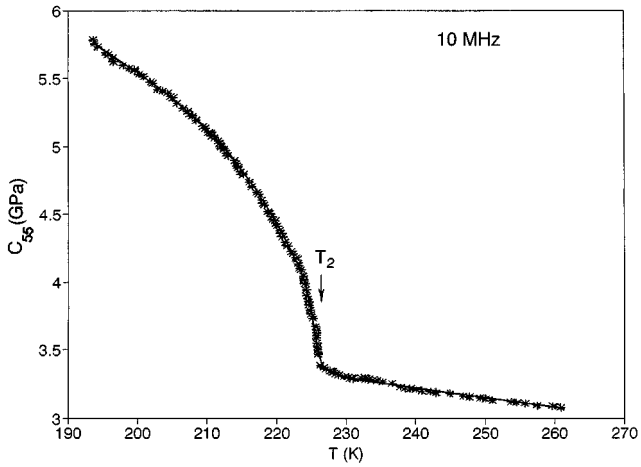

FIG. 3. Temperature dependence of the transverse elastic constant C_{55} measured by ultrasound.

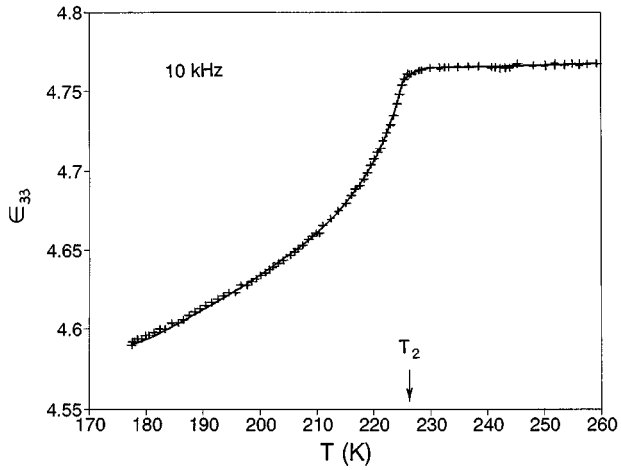

FIG. 4. Temperature dependence of the dielectric permittivity ϵ_{33}.

changes of C_{55} and ϵ_{33} at T_2 are continuous indicating that the phase transition is of second-order type.

B. Dynamical mechanical analysis (DMA 7)

The temperature dependences of the real and imaginary parts of the effective complex elastic constants $C_r^*(\mathbf{q}\|[110])$ and $C_r^*(\mathbf{q}\|[100])$ at 1 Hz are presented in Figs. 5(a) and 5(b), respectively. The changes of the effective elastic constants are associated with the temperature behavior of Young's moduli $Y([110])$ and $Y([100])$, which can be expressed through the elastic compliances S_{ij} as follows:

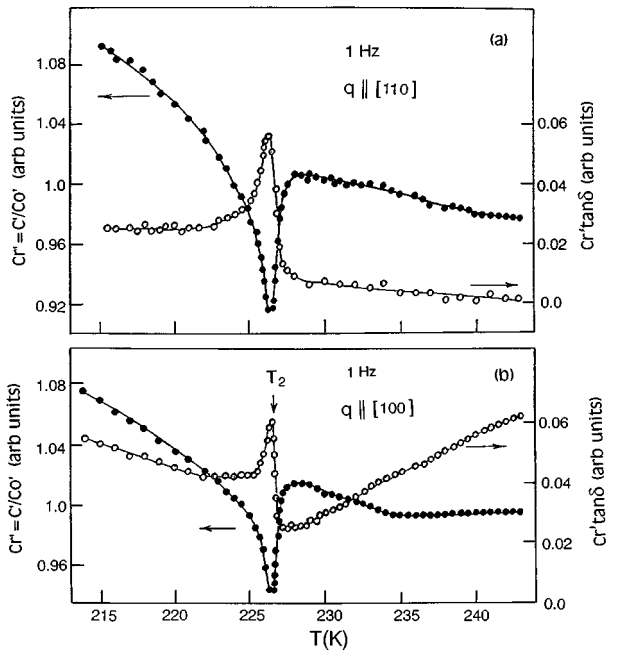

FIG. 5. Temperature dependences of the relative real $C_r'=C'/C_0$ (●) and imaginary $C_r''=C_r'\tan\delta$ (○) parts of the complex elastic constants (a) $C_r^*[110]$ and (b) $C_r^*[100]$ measured at 1 Hz.

$$Y^{-1}([100])=S_{11} \tag{2a}$$

$$Y^{-1}([110])=(S_{11}+S_{22}+S_{66}+2S_{12})/4, \tag{2b}$$

where

$$S_{11}=(C_{22}C_{33}-C_{23}^2)/\Delta, \tag{3a}$$

$$S_{22}=(C_{11}C_{33}-C_{13}^2)/\Delta, \tag{3b}$$

$$S_{12}=(C_{23}C_{13}-C_{12}C_{33})/\Delta, \tag{3c}$$

$$S_{66}=1/C_{66}, \tag{3d}$$

and

$$\Delta=C_{11}C_{22}C_{33}+2C_{12}C_{13}C_{23}-C_{22}C_{13}^2-C_{11}C_{23}^2-C_{33}C_{12}^2.$$

According to Figs. 5(a) and 5(b) both elastic constants show clear anomalous behavior in the phase transition region around T_2 in the real part as well as in the imaginary part of the complex elastic constant. This observation of a strong damping maximum at very low frequencies (1 Hz) is rather unusual. A similar behavior was measured very recently near the order-disorder phase transitions of KSCN (Ref. 7) and C_{60} (Ref. 8) and was explained in terms of a heat-diffusion central peak model. In Sec. IV we will apply this model for the discussion of the low-frequency elastic behavior of EAMC. Figures 6(a) and 6(b) show the real and imaginary parts of $C_r^*(\mathbf{q}\|[100])$ measured at various temperatures and frequencies: The magnitudes of the anomalies in the real part C_r' and in the imaginary part $C_r'\tan\delta$ of the complex elastic constant C_r^* decrease with increasing measurement frequency. The same behavior was also found for $C_r^*(\mathbf{q}\|[110])$. This unusual dispersion at ultralow frequencies will be explained in Sec. IV.

IV. DISCUSSION

Let us now consider the acoustic and dielectric properties of EAMC in the framework of the phenomenological Landau theory. The group-theoretical analysis of the phase transition D_{2h}^{18} to D_{2h}^{15} was given by Petzelt.[9] The phase transition in EAMC crystals is associated with the critical wave vector $\mathbf{k}_{15}=1/2(\mathbf{b}_1+\mathbf{b}_2)$ at the boundary of the Brillouin zone, where $\mathbf{b}_1$ and $\mathbf{b}_2$ are the reciprocal-lattice parameters and Kovalevs notation[10] has been used for the identification of wave vectors. In this case the star consists of only one wave vector ($\mathbf{k}_{15}$). All irreducible representations of the space group for this given point in the Brillouin zone are real and one dimensional. The one-component order parameter η which characterizes the phase transition transforms according to the irreducible representation $\tau_7(\mathbf{k}_{15})$ of the space group D_{2h}^{18}. The anomalous behavior of ultrasonic and dielectric properties in the region of phase transitions are usually explained on the basis of a free-energy expansion with the coupling terms, which correspond to anharmonic interactions between the deformations u_1-u_6, the polarization components P_1-P_3, and the order parameter η. This free energy has the form

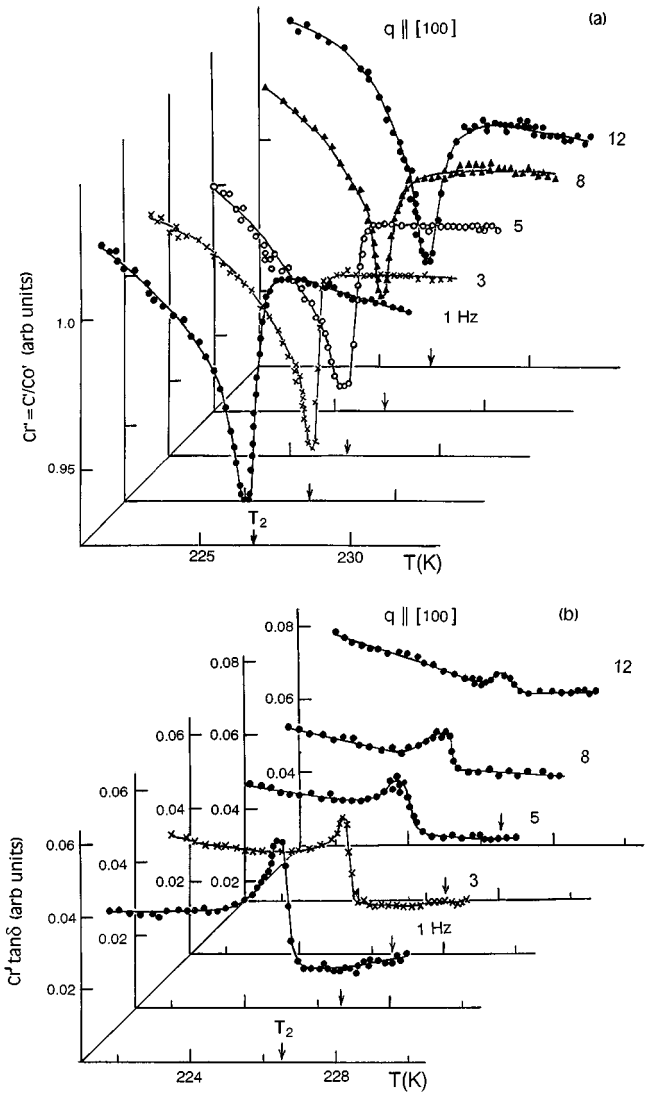

FIG. 6. Temperature dependences of the (a) relative real $C_r'=C'/C_0$ and (b) imaginary $C_r''=C_r'\tan\delta$ parts of the complex elastic constant $C_r^*[100]$ measured at various frequencies.

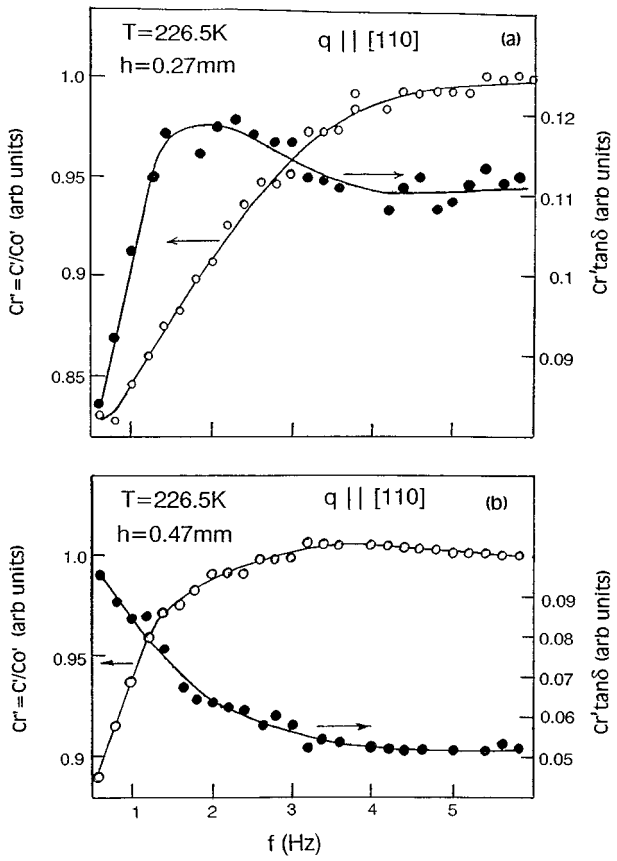

FIG. 7. Frequency dependences of the relative real $C_r'=C'/C_0$ (○) and imaginary $C_r''=C_r'\tan\delta$ (●) parts of the complex elastic constant $C_r^*[110]$ for two samples with thickness (a) $h=0.27$ mm and (b) $h=0.47$ mm.

$$F=F_\eta+F_{\eta,u}+F_{\eta,P}, \tag{4a}$$

$$F_\eta=\tfrac{1}{2}\Omega^2(k_{15})\eta^2+\tfrac{1}{4}\beta\eta^4+\tfrac{1}{6}\gamma\eta^6+\cdots, \tag{4b}$$

$$F_{\eta,u}=\sum_{i=1}^{3}a_i\eta^2u_i+\frac{1}{2}\sum_{i,j=1}^{3}b_{ij}\eta^2u_iu_j+\frac{1}{2}\sum_{j=4}^{6}b_{jj}\eta^2u_j^2, \tag{4c}$$

$$F_{\eta,P}=\frac{1}{2}\sum_{i=1}^{3}r_i\eta^2P_i^2, \tag{4d}$$

where $\Omega^2(k_{15})=A(T-T_2)$.

The changes of the complex elastic constant can be calculated from[11]

$$\Delta C_{ij}^*=\frac{\partial^2F}{\partial u_i\partial u_j}-\frac{\partial^2F}{\partial\eta\partial u_i}\chi_\eta\frac{\partial^2F}{\partial\eta\partial u_j}. \tag{5}$$

The first term in (5) contributes only to the real part of the elastic constant and is independent on the measurement frequency, while the second one displays the dynamics of the system through the wave vector and frequency dependence of the order-parameter susceptibility $\chi_\eta(\mathbf{q},\omega)$.

The interactions between the polarization components P_i $(i=1,2,3)$ and the order parameter η given in Eq. (4d) contribute only to the real part of the dielectric constant, i.e.,

$$\Delta\epsilon_{ij}=\frac{\partial^2F}{\partial P_i\partial P_j}. \tag{6}$$

To describe the observed acoustic dispersion in EAMC in the wide frequency range $f=0.5$ Hz–10 GHz (Figs. 2 and 5–7) we assume two relaxational processes which are due to order-parameter fluctuations $\delta\eta(\mathbf{q},t)=\delta\eta(\mathbf{q},0)e^{-t/\tau_\eta(\mathbf{q})}$ and temperature fluctuations $\delta T(\mathbf{q},t)=\delta T(\mathbf{q},0)e^{-t/\tau_{th}(\mathbf{q})}$. The order-parameter fluctuations lead to a relaxation mechanism in Eq. (5) of the Landau-Khlatnikov type,[11] i.e., a simple Debye form of the order-parameter susceptibility $\chi_\eta(\omega)$ with a characteristic relaxation time $\tau_\eta(q)=\tau_\eta(k_{15})/1+q^2\xi^2$, where ξ is the correlation length of the order-parameter fluctuations and $\tau_\eta(k_{15})$ is the critical relaxation time.

To describe the observed ultralow-frequency dispersion $(f=0.5-12$ Hz) in EAMC (Figs. 6 and 7) we will adopt a ''heat-diffusion central peak'' model. Such a model was quite recently developed for the explanation of the ultralow-

frequency elastic dispersion near the order-disorder phase transition in KSCN.[7] The basic idea is the following: Because of the $\eta^2 T$ coupling in the free energy (4b) the order-parameter fluctuations lead to a term $\eta_0(\mathbf{k}_{15})\delta\eta(\mathbf{k}_{15}-\mathbf{q})\delta T(\mathbf{q})$ creating a spectrum of temperature fluctuations $\delta T(\mathbf{q})$ which propagate with characteristic diffusion times

$$\tau_{\rm th}(\mathbf{q})=(\mathbf{q}\mathbf{D}_{\rm th}\mathbf{q})^{-1}, \tag{7}$$

where $\mathbf{D}_{\rm th}$ is the thermal diffusivity tensor.

In a given experiment a particular $\mathbf{q}$ component of the temperature fluctuations is probed. In an ultrasonic experiment $q=10^3$ cm^{-1} and $\tau_{\rm th}(q)\approx 10^{-3}$ s. Thus for ultrasonic frequencies ($f=10-100$ MHz) $\omega\tau_{\rm th}\gg 1$, implying that the adiabatic elastic constants are measured. The same is true for Brillouin scattering experiments. A quite different situation occurs for DMA measurements. In a three-point bending geometry (Fig. 1) the stress profile in the x direction can be approximated by $\sigma(x)\propto\cos(qx)$, where $q=\pi/h\approx 50$ cm^{-1} for $h=0.6$ mm. This leads to $\tau_{\rm th}\approx 0.12$ s. Thus for $f\ll 1$ Hz ($\omega\tau_{\rm th}\ll 1$) the isothermal elastic constant is measured whereas for $f\gg 1$ Hz ($\omega\tau_{\rm th}\gg 1$) the adiabatic one is determined. Solving the equations of motion for the order-parameter fluctuations, the strain fluctuations, and adding the heat conduction equation,[7,12] one obtains the wave vector and frequency-dependent elastic constant as

$$C_{ll}^{*}(\mathbf{q},\omega)=C_{ll}^{0}-\frac{4a_1^2\eta_0^2}{\Omega^2[1-i\omega\tau_\eta(\mathbf{q}-\mathbf{k}_{15})]}-(C_{ll}^{\rm ad}-C_{ll}^{\rm is})\frac{i\omega\tau_{\rm th}(\mathbf{q})}{1-i\omega\tau_{\rm th}(\mathbf{q})}+b_{ll}\eta_0^2, \tag{8}$$

where the difference between the adiabatic and the isothermal elastic constant is

$$C_{ll}^{\rm ad}-C_{ll}^{\rm is}=\frac{C_{lk}^0 C_{il}^0\alpha_k\alpha_i T}{C^{\epsilon}}, \tag{9}$$

α_k are the thermal expansion coefficients and C^{ϵ} is the isochoric specific heat.

Equation (8) describes two relaxational processes: The second term is due to the order-parameter fluctuations, i.e., $\delta\eta(\mathbf{q}-\mathbf{k}_{15},t)$ and the third one is due to the temperature fluctuations $\delta T(\mathbf{q},t)$. The last term in Eq. (8) originates from the η^2u^2 coupling in the free energy (4c) and leads to an elastic anomaly which is independent of the measurement frequency.

As already mentioned above the temperature fluctuations are much slower as compared to the order-parameter fluctuations, i.e., $\tau_{\rm th}\gg\tau_\eta$. In such a case the contributions of $\tau_{\rm th}$ and τ_η in Eq. (8) can be well separated: At sufficiently low measurements frequencies $\omega\tau_{\rm th}\ll 1$ and $\omega\tau_\eta\ll 1$, and the isothermal elastic constant is measured which displays the full elastic anomaly [Figs. 5(a) and 5(b)]

$$\Delta C_{ll}=-\frac{4a_l^2\eta_0^2}{\Omega^2}+b_{ll}\eta_0^2. \tag{10}$$

Increasing the measurement frequency one approaches the region $\omega\tau_{\rm th}\approx 1$ and $\omega\tau_\eta\ll 1$ [Figs. 6(a), 6(b), 7(a), and 7(b)]. In this limit one obtains

$$C_{ll}^{*}(\mathbf{q},\omega)=C_{ll}^{0}-\frac{4a_l^2\eta_0^2}{\Omega^2}-(C_{ll}^{\rm ad}-C_{ll}^{\rm is})\frac{i\omega\tau_{\rm th}(\mathbf{q})}{1-i\omega\tau_{\rm th}(\mathbf{q})}, \tag{11}$$

a simple Debye-relaxational behavior with a characteristic relaxation time $\tau_{\rm th}(\mathbf{q})$.

Increasing further the frequency one reaches the adiabatic limit $\omega\tau_{\rm th}\gg 1$ and $\omega\tau_\eta\ll 1$ and the elastic anomaly has decreased [Figs. 6(a), 7(a), and 7(b)] yielding

$$\Delta C_{ll}(\mathbf{q},\omega)=-\frac{4a_1^2\eta_0^2}{\Omega^2}+(C_{ll}^{\rm ad}-C_{ll}^{\rm is}). \tag{12}$$

At very high frequencies one approaches the region $\omega\tau_\eta\approx 1$ and the elastic anomaly reads

$$\Delta C_{ll}^{*}(\mathbf{q},\omega)=-\frac{4a_l^2\eta_0^2}{\Omega^2[1-i\omega\tau_\eta(\mathbf{q}-\mathbf{k}_{15})]}+b_{ll}\eta_0^2. \tag{13}$$

Equation (13) describes the elastic anomaly in the presence of a relaxational behavior of the order parameter. Increasing further the measurement frequency one arrives at $\omega\tau_\eta\gg 1$ and the elastic anomaly due to the $\eta^2\epsilon$ coupling [first term in (13)] vanishes completely, i.e.,

$$\Delta C_{ll}(\mathbf{q},\omega)=b_{ll}\eta_0^2. \tag{14}$$

Contrary to the longitudinal elastic constants, the transverse ones C_{jj} ($j=4,5,6$) and the dielectric permittivities ϵ_{ii} ($i=1,2,3$) are influenced by the couplings of the type η^2u^2 and η^2P^2, respectively, leading to

$$\Delta C_{55}=\mathrm{Re}\Delta C_{55}^{*}=b_{55}\eta_0^2, \tag{15a}$$

$$\Delta\alpha_{55}=\omega\ \mathrm{Im}\frac{\delta C_{55}^{*}}{2C_{55}}=0, \tag{15b}$$

$$\Delta\epsilon_{33}=r_3\eta_0^2. \tag{15c}$$

According to Eqs. (15a)–(15c) the anomalous changes in C_{55} and ϵ_{33} in the γ phase are proportional to the square of the order parameter, i.e., η_0^2, and independent of the measurement frequency. Consequently clear kinks in $C_{55}(T)$ (Fig. 3) and $\epsilon_{33}(T)$ (Fig. 4) appear in the region of T_2, while the corresponding losses are absent here.

Using the ultrasonic data for ΔC_{33} [Fig. 2(a)] and the anomalous part of the attenuation $\Delta\alpha_{33}$ [Fig. 2(b)] we have determined with Eq. (13) the order-parameter relaxation time τ_η in EAMC crystals as $\tau_\eta=\tau_0/(T_2-T)$, with $\tau_0=4.5\ 10^{-10}$ s K. Thus for ultrasonic frequencies (15 MHz) $\omega_{\rm US}\tau_\eta<1$ and $\omega_{\rm US}\tau_{\rm th}>1$ at temperatures $T_2-T>0.04$ K implying that the adiabatic anomaly is measured given by Eq. (12). For Brillouin scattering (10 GHz) $\omega_{\rm BS}\tau_\eta>1$ in a broad temperature range $T_2-T<27$ K and therefore no softening in C_{33} can be observed. Then according to Eq. (14) the anomaly in C_{33} below T_2 should be proportional to $b_{33}\eta_0^2(T)$. This is in very good agreement with the Brillouin scattering data [see also Fig. 2(a)].[4]

In the following we will corroborate that the low-frequency relaxations in EAMC are really due to the entropy fluctuations: In our three-point bending experiment an inhomogeneous stress $\sigma(\mathbf{x})\propto\cos q_x x+\sin q_z z$ is applied (Fig. 1),

where the wave vector **q** is determined by the size of the sample, i.e., $\mathbf{q}=(\pi/h,0,\pi/L)$. Then, according to Eq. (7), the thermal relaxation time $\tau_{\rm th}(\mathbf{q})$ should strongly depend on the size of the sample. Taking a usual value of $D_{\rm th}\approx 10^{-3}$ $\rm cm^2/s$ one obtains $\tau_{\rm th}(q_z)=27$ s for $L=0.5$ cm and $\tau_{\rm th}(q_x)=0.07$ s and 0.2 s for $h=0.27$ and 0.47 mm, respectively. Figure 7 shows the frequency dependences of the real and imaginary parts of the complex elastic constant near T_2 measured for those two different sample thicknesses. The damping maximum for $h=0.27$ mm at $f=2$ Hz leads to $\tau_{\rm th}=1/\omega=0.08$ s in good agreement with the above estimation for $\tau_{\rm th}(q_x=\pi/h)\approx 0.07$ s. In addition Fig. 7 clearly shows the size $(=q)$ dependence of the thermal relaxation time. For the sample with $h=0.47$ mm the damping maximum is clearly shifted to a lower frequency and as a consequence it was not measurable in this experiment. According to our rough estimation from above the damping maximum for a sample with $h=0.47$ mm should appear at $f=0.7$ Hz.

The temperature fluctuations along the long axes of the bar should show up in a damping maximum at $f=0.006$ Hz which cannot be detected by DMA-7. On the other hand, the order-parameter relaxation time in Eq. (13) is given by

$$\tau_\eta(\mathbf{q}-\mathbf{k}_{15})=\frac{\tau_\eta(\mathbf{k}_{15})}{1+q^2\xi^2}, \tag{16}$$

where ξ is the correlation length of the order-parameter fluctuations. Since for our small wave vector $q\xi\ll 1$, the order-parameter relaxation time cannot depend on the wave vector **q**. Since we have measured a pronounced **q** dependence of the slower relaxation process we can conclude that the ultralow frequency dispersion in EAMC is due to temperature fluctuations along the x direction of our sample.

The faster relaxation process in the GHz region is indeed due to the order-parameter fluctuations.

V. SUMMARY

We have measured the anomalous elastic behavior of EAMC with the ultrasonic method ($f=15$ MHz) and with low-frequency ($f=0.5-12$ Hz) dynamic mechanical analysis around the structural phase transition at $T_2=226$ K. We described our data using a phenomenological model which includes both the effect of order-parameter relaxation with a characteristic time τ_η and temperature fluctuations with a characteristic time $\tau_{\rm th}$. It turns out that the anomaly in the longitudinal elastic constants around T_2 depends strongly on the measurement frequency. At sufficiently low frequencies $f<2$ Hz the isothermal elastic constant $(\omega\tau_{\rm th}\ll 1)$ is measured, yielding the full elastic anomaly due to the $\eta^2\epsilon$ coupling in the Landau-Ginzburg free energy. At ultrasonic frequencies ($f=15$ MHz) the elastic anomaly decreased due to the isothermal-adiabatic crossover $(\omega\tau_{\rm th}\gg 1)$. In the MHz region the order-parameter relaxations can follow the strain variations $(\omega\tau_\eta\ll 1)$ leading to dip anomalies in the real and imaginary parts of the complex elastic constant. In Brillouin scattering measurements the frequency ($f=10$ GHz) is too high-for the order-parameter relaxations to follow $(\omega\tau_\eta\gg 1)$ and the negative dip anomaly at T_2 vanishes completely. This explains the absence of the negative dip anomaly observed in previous Brillouin scattering measurements of C_{33}.[4]

Thus EAMC is a unique example where the temperature fluctuations and the order-parameter relaxations can be observed with frequency-dependent elastic measurements.

ACKNOWLEDGMENTS

Two authors (A.V.K. and V.P.S.) are grateful for support from the Österreichischen Bundesministerium für Wissenschaft und Forschung. The present work was supported by the Österreichischen Fonds zur Förderung der wissenschaftlichen Forschung under Project No. P10924-PHY.

*On leave from: Institute of Physical Optics, Dragomanova str. 23, 290005, Lviv, Ukraine.

[1] V. P. Gnezdilov, V. V. Eremenko, V. S. Kurnosov, and V. I. Fomin, Sov. J. Low Temp. Phys. **15**, 667 (1989).

[2] R. Kind and P. Muralt, in *Incommensurate Phases in Dielectrics 2*, edited by R. Blinc and A. P. Levanyuk (North-Holland, Amsterdam, 1986), p. 301.

[3] S. V. Zherlitsyn, A. A. Stepanov, V. D. Fil', and V. P. Popov, Sov. J. Low Temp. Phys. **15**, 712 (1989).

[4] E. Käräjämäki, R. Laiho, T. Levola, W. Kleemann, and F. J. Schäfer, Physica B **111**, 24 (1981).

[5] E. P. Papadakis, J. Acoust. Soc. Am. **42**, 1405 (1967).

[6] B. W. Rossister and R. C. Baetzold, Phys. Meth. Chem. VII, 16 (1991).

[7] W. Schranz and D. Havlik, Phys. Rev. Lett. **73**, 2575 (1994).

[8] W. Schranz, A. Fuith, P. Dolinar, H. Warhanek, H. Kuzmany, and M. Haluska, Phys. Rev. Lett. **71**, 1561 (1993).

[9] J. Petzelt, J. Phys. Chem. Solids **36**, 1005 (1975).

[10] O. V. Kovalev, *Irreducible Representations of the Space Groups* (Gordon and Breach, New York, 1965).

[11] W. Rehwald, Adv. Phys. **22**, 721 (1973).

[12] W. Schranz, D. Havlik, and M. Fally, Mod. Phys. Lett. B (to be published).